GSTAR Satellite Disturbance from Plume Impingement

S. A. Parvez*
GTE Spacenet, McLean, Virginia

During north-south stationkeeping maneuvers on 3-axis stabilized satellites (such as the RCA Series 3000), the plume from north face thrusters used for maneuvers impinges on the north solar arrays. This results in disturbance torques along the satellite roll, yaw, and pitch axes, along with the attendant coupling of north/south velocity into the east/west direction. The disturbance torques vary as a function of the array plane orientation with respect to the active north face thruster location. Hence, the plume disturbance levels during north/south maneuvers vary with time of the year. This paper uses the data available from an operational GSTAR satellite to compute the actual disturbance torques experienced during north/south maneuvers due to plume impingement on solar array, as a function of the array position. The analysis shows that roll and yaw disturbance torques go through a complete cycle as the array position during north/south burns goes through one complete rotation, whereas the pitch disturbance torque goes through two cycles. The maximum roll and yaw disturbance torque has an approximate magnitude of 0.10 in.-lb-f (0.011 Nm), whereas the maximum pitch disturbance torque has a magnitude of 0.04 in.-lb-f (0.005 Nm). The analysis also indicates that the solar arrays may be bent in the direction of the sun.

Nomenclature

A = a constant used in the plume density curve fit equation
$F_n(F_t)$ = normal (tangential) force per unit area acting on the surface in the plume flowfield
M = molecular weight of gas under consideration
m = total mass flow rate through the jet
R = specific gas constant (ideal gas constant divided by the molecular weight of gas under consideration)
r = radial distance from the jet to the point of interest on the surface in the flowfield
T_w = temperature of the surface in the plume flowfield
T_0 = stagnation temperature of the gas
U = plume flow velocity
U_l = limiting velocity of the plume flow
β_0 = ratio of thermal velocity to freestream velocity U_l for the reflected plume flow
γ = specific heat ratio
θ = angle of incidence of the plume flow on the surface of interest
θ_l = limiting turning angle for inviscid flow at the jet nozzle exit Mach number
ρ = plume flowfield density
$\sigma_n(\sigma_t)$ = normal (tangential) accommodation coefficient
Ω_{eff} = source flow solid angle

Introduction

THE GSTAR satellites are three-axis stabilized bias-momentum spacecraft. Electrothermal hydrazine thrusters (EHT), with a nominal thrust level of 0.08 lbf (0.36 N) each, located on the north face of these spacecraft are used for north/south stationkeeping maneuvers. Of the four available EHTs (thrusters 13, 14, 15, and 16 in Fig. 1), one of two diagonally opposing pairs is chosen for any particular maneuver. Figure 1a also shows that the plume from the active EHTs would impinge on the north solar array panel, which is located right over them. This plume impingement is the primary cause of roll, yaw, and pitch disturbance torque on the spacecraft, although the combination of thrusters 13 and 15, or 14 and 16 would always result in a roll error of at least -0.05 in.-lb-f (-0.006 Nm) due to mismatch in the moment arm about the Y-axis (see Table 1). There is also a smaller contribution to disturbance torque from sources that are not calibrated on the ground, such as spacecraft mass imbalance, thruster misalign-

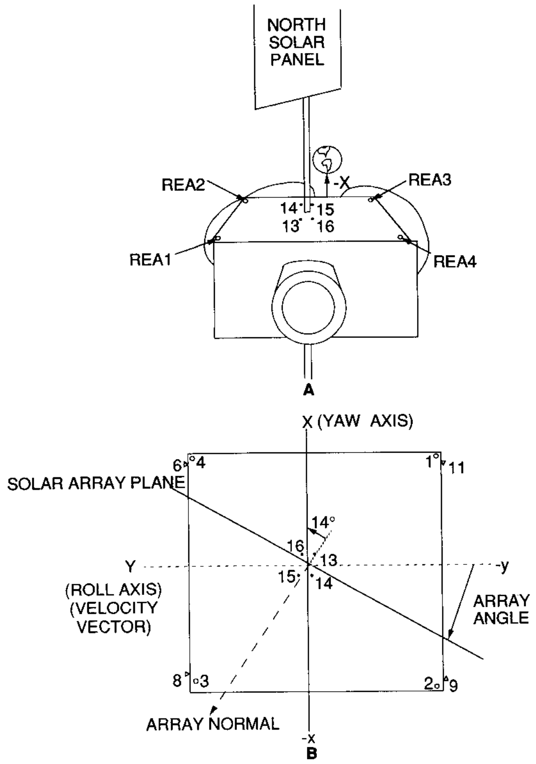

Fig. 1 Orientation of solar arrays and EHT locations.

Presented as Paper 89-0351 at the AIAA 27th Aerospace Sciences Meeting, Reno, NV, Jan. 9-12, 1989; received Jan. 16, 1989; revision received Aug. 10, 1989.

*Staff Engineer. Senior Member AIAA.

Table 1 Location and direction of north-face thrusters

Thruster No.	Moment arm, in. X	Y	Z	Direction cosine 1	2	3
1	33.2	27.2	0.77	0.0241	−0.0012	−0.9997
2	33.2	−27.6	0.84	0.0262	0.0010	−0.9997
3	−33.0	−27.6	−0.84	0.0271	−0.0020	−0.9996
4	−33.0	27.2	−0.90	0.0282	0.0010	−0.9996
13	1.23	3.91	−0.02	−0.2079	0.0542	−0.9766
14	1.18	−4.23	−0.02	0.1755	0.0530	−0.9830
15	−1.02	−4.23	0.05	0.1757	0.0544	−0.9829
16	−1.00	3.84	0.00	−0.2093	−0.0541	−0.9764

ments, and thrust level mismatch. All of these disturbance torques have to be countered by the attitude control system.

The roll and yaw control is provided by the four hydrazine thrusters, also located on the north face of the spacecraft (thrusters 1, 2, 3, and 4 in Fig. 1b), which on-pulse to provide the required control torque. The pitch control is provided by a combination of momentum wheel speed change and thrust pulses provided by thrusters 6, 8, 9, or 11 located on the east or west panel of the spacecraft (Fig. 1b). The momentum wheel, which provides a momentum level of 475 in.-lb-s (53.64 Nm-s) at the nominal wheel speed of 6000 rpm, speeds up or down to provide the pitch control torque, whereas the appropriate pitch control thruster on-pulses to provide additional control torque.

Solar Array Position and In-Orbit Data

Since the general aim of the inclination correction strategy is to reset the right ascension of the ascending node from about 90 deg to about 270 deg, the time of day for a north/south maneuver would vary with the time of the year (e.g., around spacecraft at noon during summer solstice, around midnight during winter solstice). Hence, the solar array position during north/south burn, relative to the EHT locations, would vary as a function of time of the year, essentially covering 360 deg over a year. It should also be noted that at a given time on a given day, the array angle can vary considerably, depending on the power requirement at the time.

The duty cycle data for yaw and roll control thrusters and pitch control thrusters as well as the change in momentum level corresponding to the solar array positions during north/south maneuvers are available from spacecraft telemetry. These data are used to determine the disturbance levels during spacecraft maneuvers.

Yaw and Roll Disturbance

The duty cycles on thrusters 1–4 can be converted into net roll and yaw disturbance since the control torque available from each of these thrusters is known. There is plume impingement on solar arrays from these control thrusters as well. Therefore, their control capabilities are also a function of the array position, and to impart the same torque, different duty cycles are required for the individual thrusters. Figure 2 shows the duty cycle of thrusters 1–4 during the north/south maneuvers using EHTs 13 and 15 as a function of the solar array position. As expected, the duty cycles on the individual control thrusters vary with array position, with a maximum duty cycle of 3% for any one thruster.

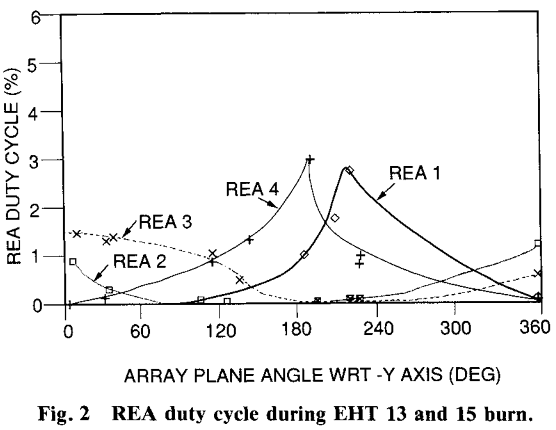

Fig. 2 REA duty cycle during EHT 13 and 15 burn.

The roll and yaw disturbances during EHT burns are due to plume impingement on solar arrays, mismatch in EHT moment arms, thruster misalignments, mass imbalance, and thrust level mismatch. Firing thrusters 13 and 15 (or the pair of 14 and 16) would result in a negative roll torque of at least 0.05 in.-lb-f (0.006 Nm) due to mismatch in their respective moment arm about the roll axis (see Table 1). The large variations in disturbance as a function of the solar array position that is apparent from Fig. 3 indicates that plume impingement is the largest source of disturbance.

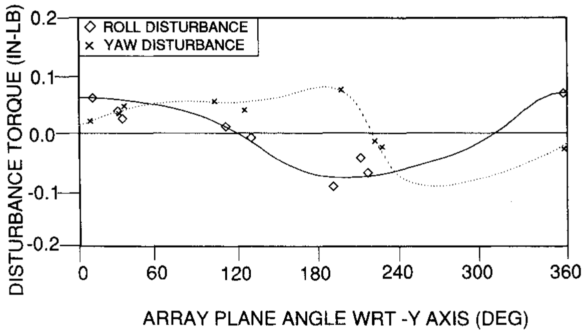

Fig. 3 Roll and yaw disturbance from firing EHT 13 and 15.

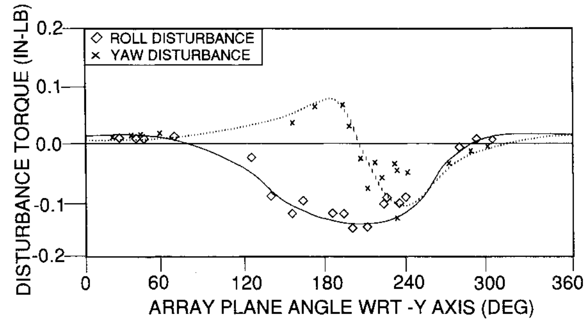

Fig. 4 Roll and yaw disturbance from firing EHT 13 and 15 after 4 yr in orbit.

Figure 3 shows the yaw torque, resulting from EHT 13 and 15 burn, going through a cycle as the solar array cycles through 360 deg with a maximum disturbance magnitude of about 0.1 in.-lb-f (0.011 Nm). Figure 3 also shows the roll disturbance for EHTs 13 and 15 going through a cycle as well but out of phase with the yaw disturbance by about 90 deg. The maximum roll torque magnitude is also about 0.1 in.-lb-f (0.011 Nm). The yaw and roll torque from the thruster plume results from the normal component of the plume force on the array surface. This force would depend on the incidence angle of the plume force on the array surface as well as the surface properties of the array such as the surface temperatures and accommodation coefficients. Therefore, even for a pair of EHTs that are perfectly symmetric about the array plane and have thrust axis parallel to the array boom, there will be a substantial net plume normal force due to difference in surface properties between the front and back of the array, resulting in yaw and roll torques. The cyclic nature of the disturbance torques shown in Figs. 3 and 4 can therefore be explained by the changing direction of the plume forces normal to the array. The change in magnitude of the disturbance is due to variation in the distances of the array surface from the active EHTs and the resultant variation in incidence angle.

Figure 3 shows the yaw and roll disturbance levels on the spacecraft. Figure 3 shows that in addition to the cyclic plume torque, there is a net negative roll torque due to the mismatch in the roll moment arm of EHTs (as discussed earlier) resulting in a bigger magnitude for negative roll torque than for positive roll torque. Figure 3 shows that the yaw and roll disturbance levels are highest when the solar array plane is in proximity to the pair of active EHTs (the solar arrays rotate around the spacecraft $-Z$ axis). The available data also show a nonsymmetrical nature on the roll and yaw disturbance cycle. This is because of the nonsymmetrical location of the EHTs, as well as the asymmetry in the plume vector direction, as may be deduced from Table 1. The solar arrays also bend over time in the direction of the sun. This phenomenon is more apparent from disturbance data on satellites that have been in orbit for a longer period of time, such as those shown in Fig. 4. The torque profile shows an increased disturbance due to plume impingement on the front of the solar array. This probably results because the array plane is bent in the direction of the sun and thereby provides a higher plume incidence angle for the front of the array. The lack of symmetry of the thruster plume vector plus the bending of the solar array can cause the nonsymmetrical nature of the roll and yaw disturbance torques apparent from the plots.

Pitch Disturbance

Pitch disturbance torque on the spacecraft can be computed by equating it to the rate of change of the momentum wheel speed and the duty cycle of the pitch control thrusters (thrusters 6, 8, 9, and 11 in Fig. 1b). The relative contribution of the momentum wheel and the thrusters in providing the pitch control torque is shown in Fig. 5. In all cases, the thrusters provide the major control, and the relative magnitude is dependent on the selection of the pitch error threshold and the thruster pulse width and pulse separation.

Pitch disturbance during EHT maneuvers is primarily due to plume impingement on the solar arrays. The disturbance levels are a function of the solar array position with respect to the active EHTs. Figure 6 shows the pitch disturbance for a burn using EHTs 13 and 15. The pitch disturbance goes through two complete cycles as the array angle rotates through 360 deg with a maximum disturbance magnitude of about 0.04 in.-lb-f (0.005 Nm).

The direction and phasing of the pitch disturbance torque can be reasonably explained by examining the array orientation with respect to EHTs 13 and 15, as shown in Fig. 1b. With array angles of 14 deg and 194 deg, the array plane is perpendicular to the line joining EHTs 13 and 15. The plume forces on the arrays from the two thrusters cancel out the disturbances, resulting in negligible pitch torque. Similarly, at array angles of 104 deg and 284 deg, the array plane would be directly over the EHTs, which should also result in negligible pitch torque. Between array angles of 14 deg and 104 deg and angles of 194 deg and 284 deg, a positive pitch torque may be expected, whereas between array angles of 284 deg and 14 deg and 104 deg and 194 deg, a negative torque may be expected. The total pitch torque would be the additive effect of the pitch torque from each of the EHTs.

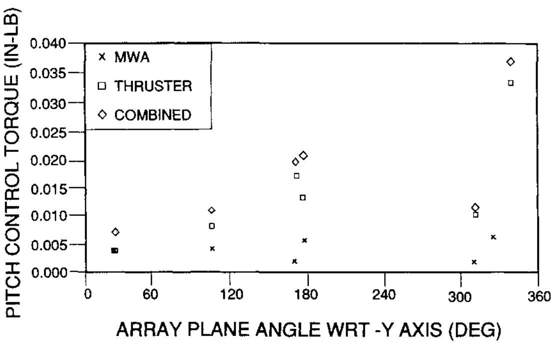

Fig. 5 Pitch control torque provided by thrusters and momentum wheel.

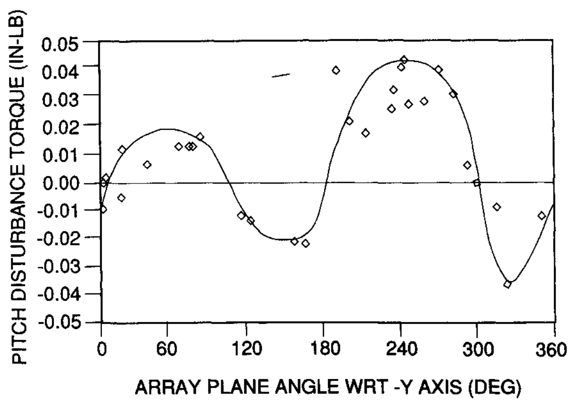

Fig. 6 Pitch disturbance from firing EHT 13 and 15.

Table 2 Parameters for EHT jet

Parameters	Values
A	0.06
$\dot{m}$	7.32×10^{-6}
θ_∞	89.85 deg
γ	1.26
R	1545 lbft/°R 1b mole
T_0	2000 °R
T_w	500 °R
Ω_{eff}	44.32 deg
U_l	6.6×10^4 in./s
ρ	5.28×10^{-15} slug/in.^{3}

The actual pitch disturbance torques shown in Fig. 6 qualitatively correspond to this prediction reasonably well. The phase difference between the prediction and the actual is caused by the different cant of the two EHTs respective to the solar arrays (as explained earlier), as well as the possible bend in the arrays themselves. These differences also result in the asymmetry in the disturbance profile.

Theoretical Prediction of Plume Torque

Reference 1 contains a theoretical determination of plume impingement on solar array from north face reaction engine assemblies (REAs) for an earlier momentum bias communication satellite. The results of that analysis, however, are not valid for GSTAR satellites due to the change in thruster type, thruster-location geometry, and the difference in array size and location. Using the method in Ref. 1, an attempt is made to theoretically determine the maximum disturbance torque resulting from plume impingement on solar arrays.

To determine the plume flowfield density, an approximate curve fit to the method of characteristics (MOC) density contour in the region of the solar arrays is

$$\rho = (\dot{m}/U_l)\,(\cos^8\theta + A\,\cos^4\theta)/r^2$$

The jet is assumed to be a source flow of solid angle Ω_{eff} defined by

$$\Omega_{\text{eff}} = 2\pi\int_0^{\theta_\infty}(\cos^8\theta + A\,\cos^4\theta)\,\sin\theta d\theta$$

Assuming the solar array to be near the centerline of the plume flow and far from the jet nozzles (large distances compared to the nozzle exit diameter), the velocity of the plume flow can be assumed to have reached the limiting value U_l defined by

$$U_l = \sqrt{2\gamma R T_0/(\gamma - 1)M}$$

Table 2 shows the assumed values of thruster parameters and the values calculated from the preceding equations.

To determine the plume impingement forces and the disturbance torque about the spacecraft center of mass, the assumptions of free molecular flow and very high velocity were made in Ref. 1. Using the same criteria, the plume force normal to the surface is defined by

$$F_n = \rho U^2[(2 - \sigma_n) \sin^2\theta + \sigma_n\beta_0 \sin\theta]$$

where

$$\beta_0 = \sqrt{\pi(T_w/T_0)(\gamma - 1)/4\gamma}$$

The temperature of the surface in the plume flowfield is T_w, and σ_n is the surface accommodation coefficient. Assuming one side of array to have entirely specular reflection ($\sigma_n = 0$) and the other side to have entirely diffuse reflection ($\sigma_n = 1$), the maximum yaw/roll torque is computed to be 0.05 in.-lb-f (0.006 Nm). The maximum pitch torque is computed to be 0.01 in.-lb-f (0.001 Nm).

The theoretical prediction of the maximum torques is smaller than the maximum yaw/roll torque of 0.1 in.-lb-f (0.011 Nm) seen in Fig. 3 and the maximum pitch torque of 0.04 in.-lb-f (0.005 Nm) seen in Fig. 6. Most of this discrepancy can be explained by the fact that the theoretical model assumed thrust vector perfectly parallel to the array boom and also assumed a solar array without any distortions. Since the plume force on the arrays is very sensitive to the angle of incidence, a difference of 1 deg in the effective incidence angle (due to bending of arrays, etc.) can result in a net change of about 0.03 in.-lb-f (0.003 Nm) in yaw/roll torque. It has already been noted earlier that the EHTs have different cant angles and that the array plane have distortions. Errors in other assumptions for theoretical modelling would account for any remaining discrepancy. Reference 1 also indicates that its theoretically derived value had to be doubled to match the actual disturbance levels.

Conclusion

This study shows considerable disturbance torque on a three-axis stabilized spacecraft during north/south maneuvers due to plume impingement on the north solar array. The disturbance torques are cyclical in nature depending on array plane location respective to the active thrusters. There is also a negative bias in roll torque due to mismatch in the moment arm of the two EHTs. Roll and yaw disturbance go through one cycle as the array position goes through 360 deg, whereas the pitch disturbance goes through two complete cycles. The maximum roll and yaw disturbance torque is 0.1 in.-lb-f (0.011 Nm), and the maximum pitch torque is about 0.04 in.-lb-f (0.005 Nm). A simple theoretical model predicted a smaller disturbance for both.

The actual disturbance torques calculated in this paper from the on-orbit data can be used to validate the plume models used in the spacecraft design phase for predicting the disturbance. These results may also be used to set up the appropriate control parameters to compensate for the expected disturbances during maneuvers and also to design attitude control systems on future spacecraft.

Pitch disturbance during north/south maneuvers has a significant implication in the east/west stationkeeping of satellites. Since the pitch control thrusters are located on the east and west faces of the spacecraft, thruster activity for pitch control will provide a velocity change in the east/west direction during the north/south maneuvers, and the coupling of these can be appreciable for spacecraft such as GSTAR I and GSTAR II, which are located near the equilibrium longitudes.[2] The analysis shown in this paper, in conjunction with Ref. 3, can be used to determine the appropriate choice of pitch control thrusters and the overall strategy in planning for coupling from north/south maneuvers.

References

[1]Fox, S. M., "Effects of Plume Impingement on a Momentum Bias Communication Satellite," *Journal of Spacecraft and Rockets,* Vol. 20, No. 1, 1983, pp. 55–60.

[2]Parvez, S., and Pardo, J., "East/West Stationkeeping Near An Equilibrium Longitude at 105 Degrees West," *Advances in Astronautical Sciences,* Vol. 65, American Astronomical Society, Washington, DC, pp. 1555–1566.

[3]Pardo, J., "North/South Coupling Study," *Advances in Astronautical Sciences,* Vol. 65, American Astronomical Society, Washington, DC, pp. 1567–1583.

James A. Martin
Associate Editor